Supplementary Information

Synthesis and Characterization of Single-Crystal $Cu(In,Ga)Se_2$ Nanowires: High Ga Contents and Growth Behaviour

J. Y. Lee,[a,b,1] W. K. Seong,[a,1] J.-H. Kim,[a] S.-H. Cho,[a] J.-K. Park,[a] K.-R. Lee,[a] M.-W. Moon,[a] and C.-W. Yang[c**]*

[a]Institute for Multi-Disciplinary Convergence of Matter, Korea Institute of Science and Technology (KIST), Seoul 130-650, Republic of Korea
[b]Advanced Analysis Center, Korea Institute of Science and Technology (KIST), Seoul 130-650, Republic of Korea
[c]School of Advanced Materials Science and Engineering, Sungkyunkwan University, Suwon 440-746, Republic of Korea

To whom correspondence should be addressed. E-mail: [*]mwmoon@kist.re.kr, [**]cwyang@skku.edu.

Supplementary Figures

1. Schematic diagram of the thermal CVD process for synthesizing the CIGS NWs

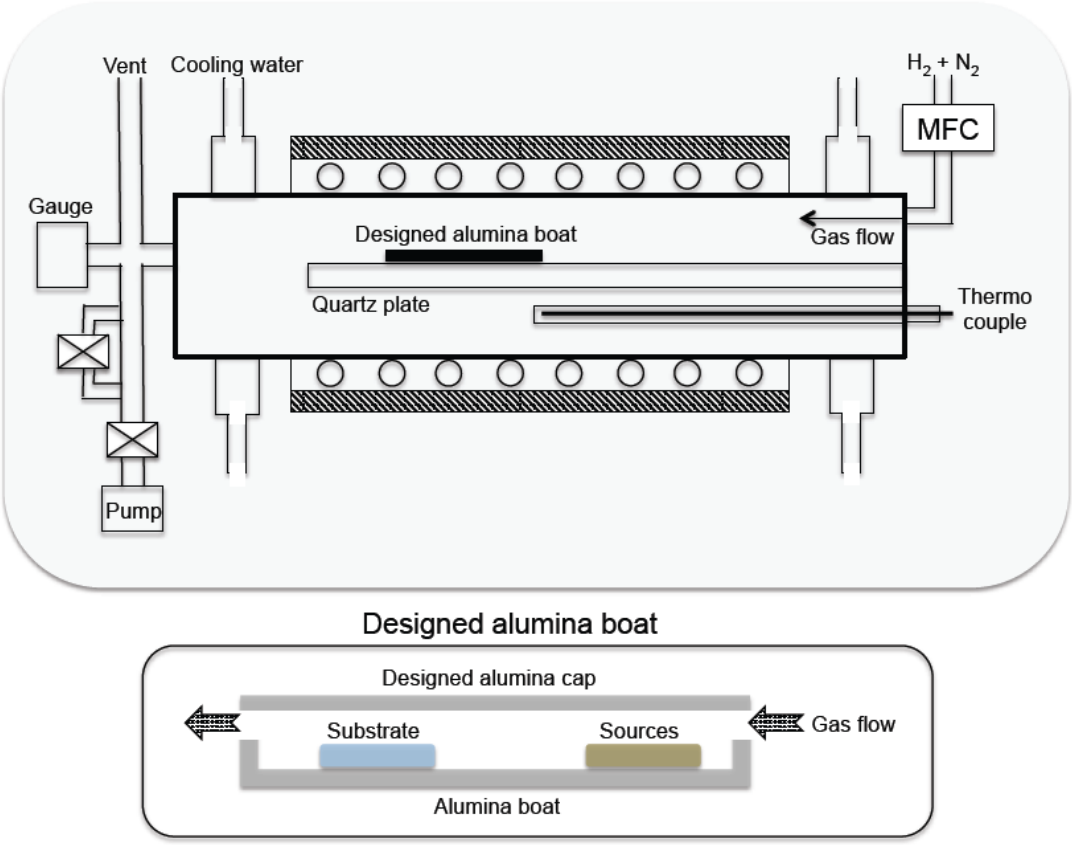

Fig. S1. Experimental setup used for the synthesis of the CIGS NWs.

2. FE-SEM micrographs of the freestanding and horizontally grown CIGS NWs

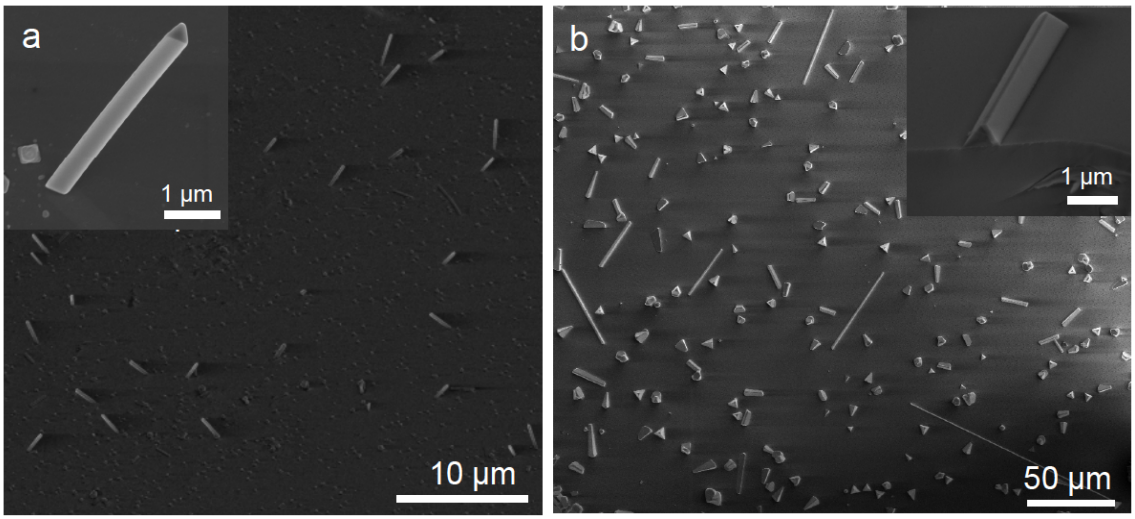

Fig. S2. Plane-view FE-SEM micrographs of the (a) freestanding and (b) horizontally grown CIGS NWs on an *r*-cut Al_2O_3 substrate. The insets show tilted cross-sectional views of individual NWs.

Under a low-deposition flux, the diameters and lengths of the freestanding CIGS NWs are approximately 50–700 nm and 1–20 μm, respectively, while that of the horizontally grown CIGS NWs on the *r*-cut Al_2O_3 substrate are approximately 500–1500 nm and 1–100 μm, respectively. As shown in the insets of Figs. S2(a) and (b), the CIGS NWs have well-defined facets at the tip and sidewalls, with the NWs exhibiting a triangular cross section.

3. A HR-TEM micrograph and corresponding STEM/EDS results for a freestanding CIGS NW

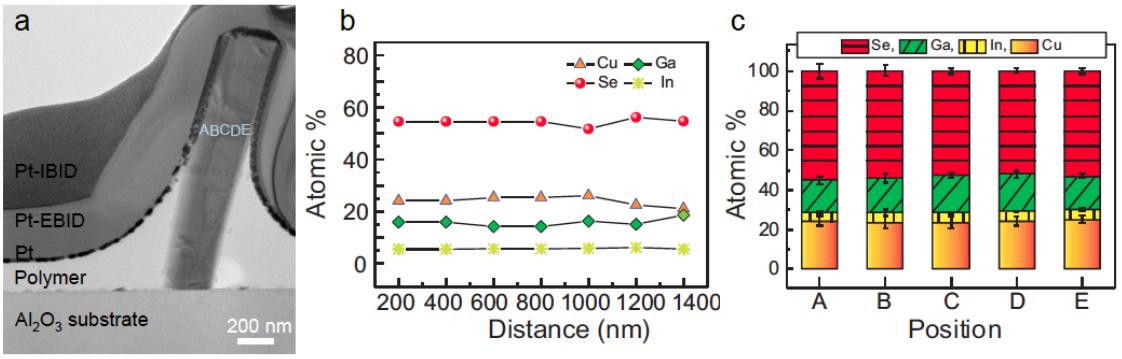

Fig. S3. (a) A cross-sectional TEM micrograph of a freestanding CIGS NW on the *r*-cut Al_2O_3 substrate. Pt and a commercial epoxy were used to protect the surface of the NW during the sample preparation. (b) and (c) are the STEM/EDS results for the atomic composition and distribution along the length and radial directions, respectively.

We also obtained information about the chemical composition of the freestanding CIGS NWs along the axial and radial directions with STEM/EDS measurements, with the results shown in Fig. S3. As shown in Figs. S3(b) and (c), the average contents of each element in both directions are 24.6 at.% of Cu, 4.9 at.% of In, 17.3 at.% of Ga, and 53.2 at.% of Se, which suggests a stoichiometry of $Cu_{1.1}(In_{0.2}Ga_{0.8})Se_{2.3}$. The Ga content ratio in the CIGS NW (0.8/(In + Ga)) is higher than that of the In content ratio (0.2/(In + Ga)). Therefore, the Cu/(In + Ga) and Ga/(In + Ga) ratios of the freestanding CIGS NWs are 1.1 and 0.78, respectively.

4. Cross-sectional TEM micrographs of a horizontal CIGS NW

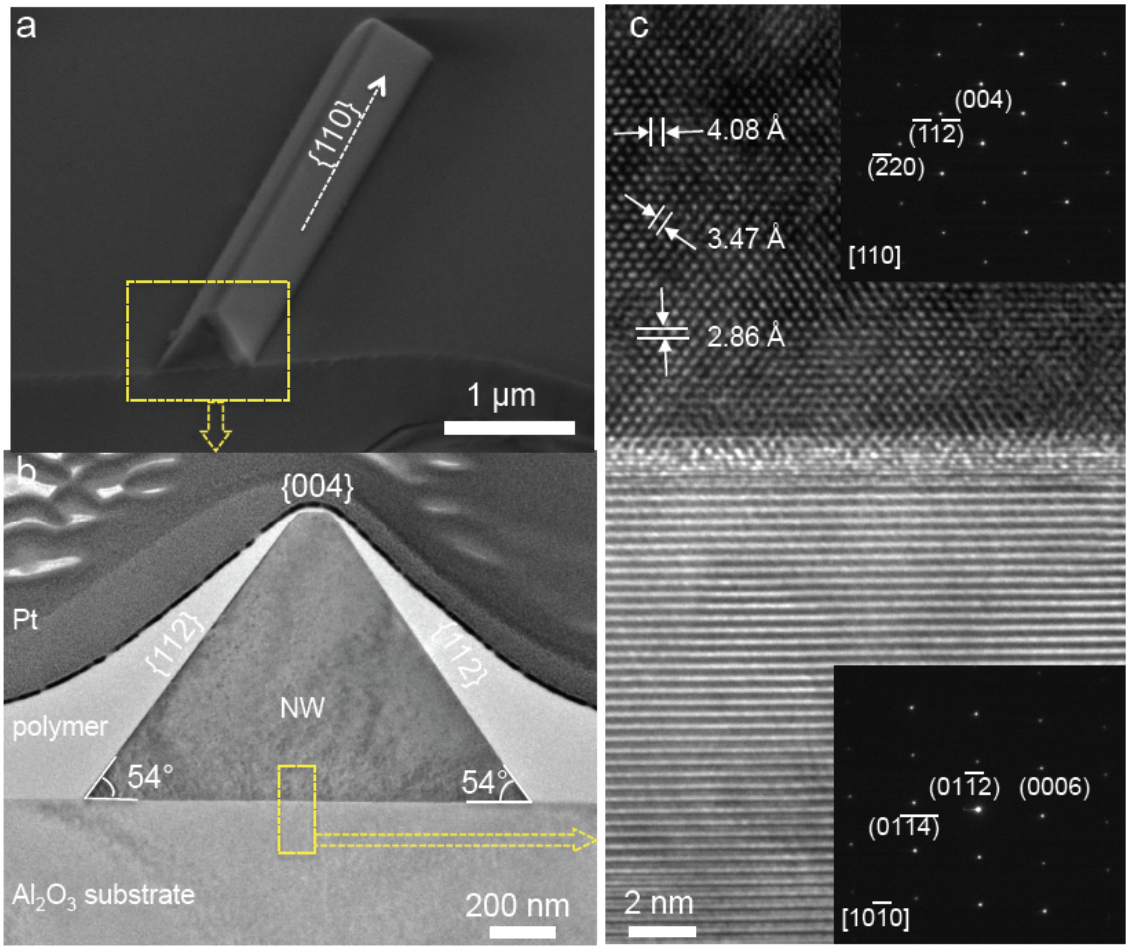

Fig. S4. (a) Cross-sectional SEM and (b) TEM micrographs of a horizontal CIGS NW grown on the *r*-cut Al_2O_3 substrate along the radial direction, which shows the truncated triangular cross section of the NW. As shown in Fig. S4(b), the angle between the sidewall of the NW and substrate is 54°. (c) A magnified HR-TEM micrograph of the interface between the CIGS NW and *r*-cut Al_2O_3 substrate. The insets are the corresponding SAED patterns.

5. Orientation relationship between the CIGS NW and *r*-cut Al_2O_3 substrate

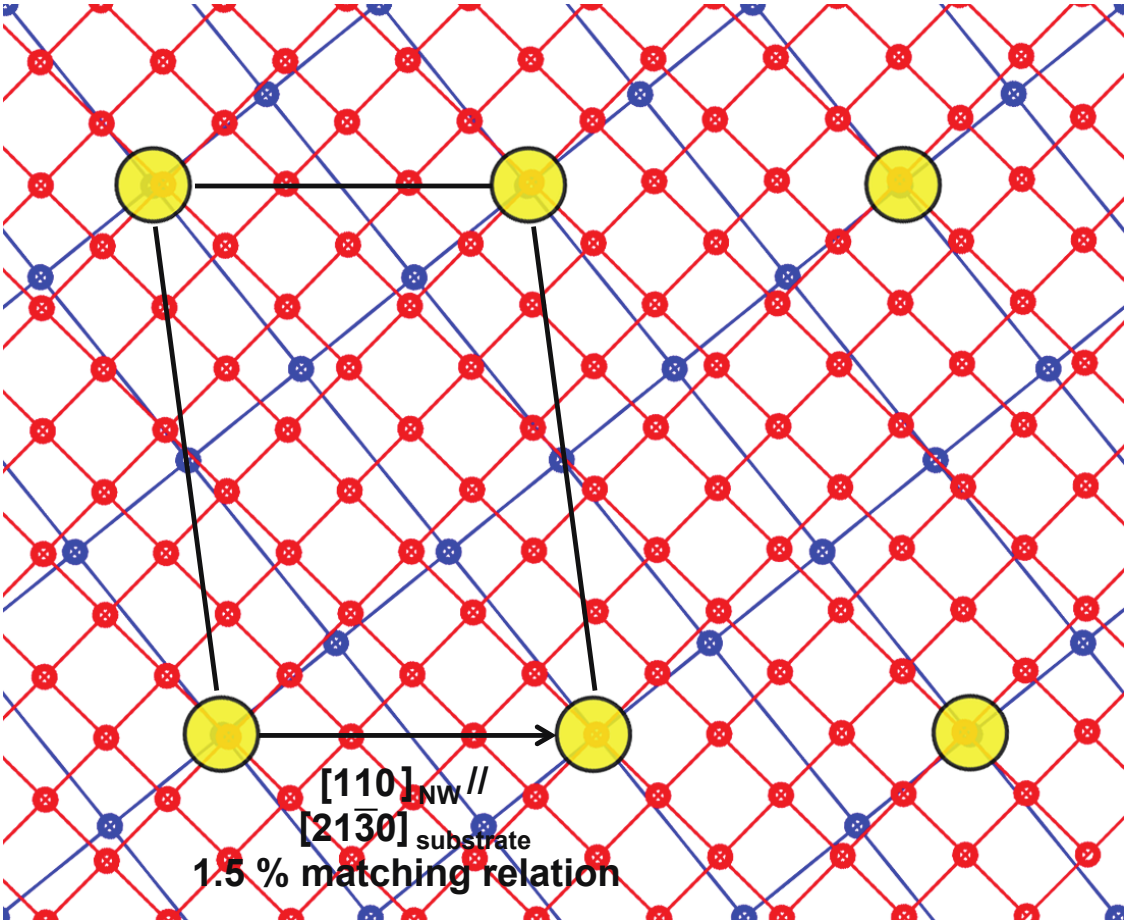

Fig. S5. The long-rang lattice matching relationship between the (004) plane of a CIGS NW (red) and the (012) plane of the Al_2O_3 substrate (blue). Their orientation relationship is $[110]_{NW}||[210]_{substrate}$. The linear mismatch between the [110] direction of the CIGS NW and the [210] direction of the *r*-cut Al_2O_3 substrate is approximately 1.5%.